

Free vibration of functionally graded carbon nanotube-reinforced composite beam

Dang Van Hieu^{*}, Nguyen Thi Kim Thoa

Thai Nguyen University of Technology.

^{*}Corresponding author: hieudv@tnut.edu.vn

Received 15 Sep. 2023; Revised 10 Nov. 2023; Accepted 15 Nov. 2023; Published 10 Dec. 2023.

DOI: <https://doi.org/10.54939/1859-1043.j.mst.FEE.2023.119-126>

ABSTRACT

The purpose of this paper is to investigate the free vibration behavior of functionally graded carbon nanotube-reinforced composite (FG-CNTRC) beam. The carbon nanotubes (CNTs) are aligned and distributed in polymeric matrix with different patterns of reinforcement. The material properties of the FG-CNTRC beam are estimated by using the rule of mixture. The trigonometric shear deformation beam theory is employed to deal with the problem. The mathematical models provided in this paper are numerically validated by comparison with some available results. New results of free vibration analyses of FG-CNTRC beam are presented and discussed in detail. The effects of the length to thickness ratio and CNT volume fraction are taken into investigation.

Keywords: Vibration; FG-CNTRC beam; Shear deformation beam theory.

1. INTRODUCTION

CNTs have been accepted as an excellent candidate for the reinforcement of polymer composites due to their high elastic modulus, tensile strength and low density. The potential applications of polymer/CNTs are found in the field of reinforcing composites, high performance structural and multifunctional composites [1, 2].

In actual applications, the CNTRCs can be incorporated into structural elements such as beams, plates and shells. CNT-based FG materials were first proposed by Shen [3] with CNT distributions within an isotropic matrix designed specifically to grade them with certain rules along the desired directions to improve the mechanical properties of the structures. A series of investigations about FG-CNTRC beams were then conducted to study the mechanical properties of nanocomposites. For example, Ke et al. [4] analyzed the nonlinear free vibration of the FG-CNTRC beams by means of the Timoshenko beam theory, using the Ritz method and direct iterative procedure. Yas and Heshmati [5] presented the dynamic response of the nanocomposite beams with randomly oriented CNTs under moving load. Stability and dynamic characteristics of the Timoshenko FG-CNTRC beams resting on the elastic foundation were carried out by Yas and Samadi [6] using the generalized differential quadrature method. Wattanasakulpong and Ungbhakorn [7] used the analytical method to analyse the bending, buckling and vibration of simply-supported FG-CNTRC beams resting on an elastic foundation. Rafiee et al. [8] studied the nonlinear thermal bifurcation buckling of FG-CNTRC beams with surface-bonded piezoelectric layers. The behaviors of large amplitude vibration, nonlinear bending and thermal postbuckling of nanocomposite beams reinforced by single-walled carbon nanotubes (SWCNTs) resting on an elastic foundation in thermal environments were investigated by Shen and Xiang [9]. In particular, recent studies on the mechanical behaviors of the FG-CNTRC structures are systematized in the review paper of Liew et al. [10].

It is known that the Euler-Bernoulli beam theory is based on the assumption that the plane section perpendicular to the neutral axis before deformation remains plane and perpendicular to the neutral axis after deformation, implying that the transverse shear and transverse normal

strains are zero. This is the reason that this theory is applicable to slender beams only. The Timoshenko beam theory is based on the assumption that the plane section perpendicular to the neutral axis before deformation remains plane but not necessarily perpendicular to the neutral axis after deformation [4-6]. In the Timoshenko beam theory, the transverse shear stress distributions are constant through the thickness and require a shear correction factor to properly account for the strain energy due to shear deformation. The limitations of the Euler-Bernoulli and Timoshenko beam theories for beams forced the development of higher-order refined shear deformation beam theories. In these theories, displacement distribution is represented by either polynomial or non-polynomial functions in terms of thickness coordinate to take into account the effects of shear deformation and does not require a shear correction factor [7]

In the present study, the free vibration of the FG-CNTRC beam is investigated using the Navier solution method. The simply-supported FG-CNTRC beam is considered. The trigonometric shear deformation beam theory is employed to solve such problem. A new solution of natural frequency is presented and discussed in detail. Several aspects of thickness ratios, CNT volume fractions, types of CNT distribution, etc., which have a considerable impact on the analytical solutions, are also investigated.

2. PROBLEM

2.1. FG-CNTRC beam

A FG-CNTRC beam made from a mixture of CNTs and an isotropic polymer matrix is considered. The beam with simply-supported on both ends, having length (L), thickness (h) and width (b), as shown in figure 1a. In this study, the beam is assumed to have four different patterns of CNTs reinforcement over the cross sections, as shown in figure 1b.

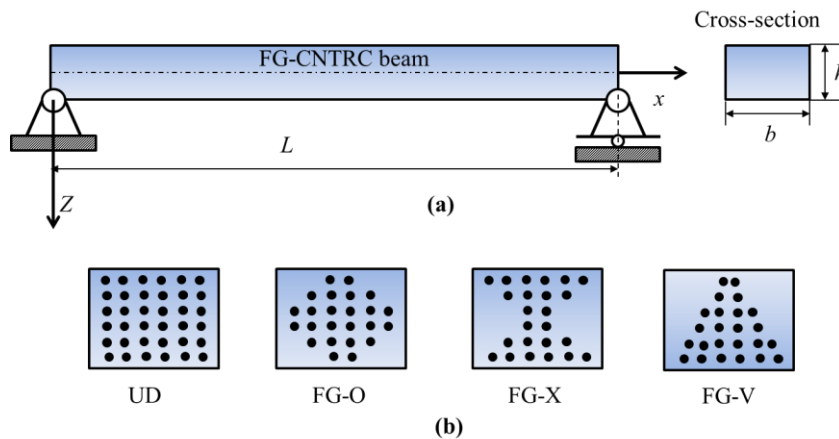


Figure 1. Geometry of a FG-CNTRC beam (a) and cross sections of different patterns of reinforcement (b).

The effective material properties of the FG-CNTRC beam can be estimated using the rule of mixture. Therefore, the expressions of the effective Young's modulus and shear modulus of CNTRC beams are as follows [3-10]:

$$E_{11} = \eta_1 V_{CNT} E_{11}^{CNT} + V_p E^p; \frac{\eta_2}{E_{22}} = \frac{V_{CNT}}{E_{22}^{CNT}} + \frac{V_p}{E^p}; \frac{\eta_3}{G_{12}} = \frac{V_{CNT}}{G_{12}^{CNT}} + \frac{V_p}{G^p} \quad (1)$$

where E_{11}^{CNT} , E_{22}^{CNT} and G_{12}^{CNT} are the Young's moduli and shear modulus of CNT, respectively; E_p and G_p are corresponding the Young's modulus and shear modulus of the polymer matrix; also, V_{CNT} and V_p are the volume fractions of the CNT and the polymer matrix, respectively. To

consider the size-dependent material properties of CNTs, the CNT efficiency parameters, η_i ($i = 1,2,3$), are introduced. They can be determined by matching the elastic moduli of CNTRCs estimated by the molecular dynamics simulation with the numerical results estimated by the rule of mixture. The Poisson's ratio (ν) and mass density (ρ) of the FG-CNTRC beam are written [7]:

$$\nu = V_{CNT}\nu^{CNT} + V_p\nu^p; \rho = V_{CNT}\rho^{CNT} + V_p\rho^p \quad (2)$$

where ν^{CNT} and ν^p are corresponding the Poisson's ratio of the CNT and the polymer matrix; and ρ^{CNT} and ρ^p are the mass densities of the CNT and the polymer matrix, respectively. For different patterns of CNTs reinforcement distributed across the cross section of the beam as shown in figure 1b, the continuous mathematical functions used for describing the distributions of material constituents are given below [6, 7]:

$$\text{UD:} \quad V_{CNT} = V_{CNT}^* \quad (3a)$$

$$\text{FG-O:} \quad V_{CNT} = 2(1 - 2|z|/h)V_{CNT}^* \quad (3b)$$

$$\text{FG-X:} \quad V_{CNT} = (4|z|/h)V_{CNT}^* \quad (3c)$$

$$\text{FG-V:} \quad V_{CNT} = (1 + 2z/h)V_{CNT}^* \quad (3d)$$

where V_{CNT}^* is the given volume fraction of CNTs, which can be obtained from the following equation:

$$V_{CNT}^* = \frac{m_{CNT}}{m_{CNT} + (\rho^{CNT} / \rho^m)(1 - m_{CNT})} \quad (4)$$

where m_{CNT} is the mass fraction of CNTs. From Eq. (3), it can be defined that the FG-O, FG-X and FG-V beams are some kinds of FG beams in which their material constituents are varied continuously across their thicknesses; while, the UD beam has uniformly distributed CNT reinforcement. In this work, the Poly methyl methacrylate (PMMA) is selected as the polymer matrix, the CNT efficiency parameters (η_i) associated with the given volume fraction V_{CNT}^* are: $\eta_1 = 1.2833$ and $\eta_2 = \eta_3 = 1.0556$ for case of $V_{CNT}^* = 0.12$; $\eta_1 = 1.3414$ and $\eta_2 = \eta_3 = 1.7101$ for case of $V_{CNT}^* = 0.17$; $\eta_1 = 1.3238$ and $\eta_2 = \eta_3 = 1.7380$ for case of $V_{CNT}^* = 0.28$ [6].

2.2. Equations of motion

Consider a trigonometric shear deformation beam theory, the displacement field can be written in the following forms [11]:

$$u_1(x, z, t) = u(x, t) - z \frac{\partial w(x, t)}{\partial t} + \Phi(z)f(x, t); u_2(x, z, t) = 0; u_3(x, z, t) = w(x, t) \quad (5)$$

where u and w are the axial and transverse displacement at the reference plane of the FG-CNTRC beam, respectively. $f(x, t) = \frac{\partial w(x, t)}{\partial x} - \phi(x)$ is transverse shear strain at any point on the reference plane. Here, $\phi(x)$ is the total bending rotation of the cross-section at any point of the reference plane and t is time. For the trigonometric shear deformation beam, the shape function is given as $\Phi(z) = \frac{h}{\pi} \sin\left(\frac{\pi z}{h}\right)$ which describes the transverse shear stress distribution across the beam thickness.

To obtain the governing equations of motion, the Hamilton's principle is employed as follows:

$$\int_{t_1}^{t_2} (\delta U - \delta K) dt = 0 \quad (6)$$

where δU is the virtual variation of the total strain energy, and δK is the virtual kinetic energy. The virtual strain energy of the beam is:

$$\begin{aligned} \delta U &= \int_0^L \int_A (\sigma_{xx} \delta \varepsilon_{xx} + \sigma_{xz} \delta \gamma_{xz}) dA dx \\ &= \int_0^L \left[N_x \frac{\partial \delta u}{\partial x} - M_x \frac{\partial^2 \delta w}{\partial x^2} + P_x \left(\frac{\partial^2 \delta w}{\partial x^2} - \frac{\partial \delta \phi}{\partial x} \right) + Q_x \left(\frac{\partial \delta w}{\partial x} - \delta \phi \right) \right] dx \end{aligned} \quad (7)$$

herein, $A = b \times h$ is the area of cross section of the beam; N_x , M_x , P_x and Q_x are the stress resultants in terms of the normal force, bending moment, higher-order generalized force and shear force, respectively; these stress resultants are defined as:

$$N_x = \int_A \sigma_{xx} dA = A_{11} \frac{\partial u}{\partial x} - B_{11} \frac{\partial^2 w}{\partial x^2} + C_{11} \left(\frac{\partial^2 w}{\partial x^2} - \frac{\partial \phi}{\partial x} \right) \quad (8a)$$

$$M_x = \int_A z \sigma_{xx} dA = B_{11} \frac{\partial u}{\partial x} - D_{11} \frac{\partial^2 w}{\partial x^2} + F_{11} \left(\frac{\partial^2 w}{\partial x^2} - \frac{\partial \phi}{\partial x} \right) \quad (8b)$$

$$P_x = \int_A \Phi(z) \sigma_{xx} dA = C_{11} \frac{\partial u}{\partial x} - F_{11} \frac{\partial^2 w}{\partial x^2} + H_{11} \left(\frac{\partial^2 w}{\partial x^2} - \frac{\partial \phi}{\partial x} \right) \quad (8c)$$

$$Q_x = \int_A \frac{d\Phi(z)}{dz} \sigma_{xz} dA = A_{55} \left(\frac{\partial w}{\partial x} - \phi \right) \quad (8d)$$

where

$$[A_{11}, B_{11}, D_{11}] = \int_A \frac{E_{11}(z)}{1-\nu^2(z)} [1, z, z^2] dA; [C_{11}, F_{11}] = \int_A \frac{E_{11}(z)}{1-\nu^2(z)} \Phi(z) [1, z] dA \quad (9a)$$

$$H_{11} = \int_A \frac{E_{11}(z)}{1-\nu^2(z)} \Phi^2(z) dA; A_{55} = \int_A G_{12}(z) \left[\frac{d\Phi(z)}{dz} \right]^2 dA \quad (9b)$$

The virtual kinetic energy (δK) takes the form:

$$\delta K = \int_0^L \left\{ \begin{aligned} &I_0 (\dot{u} \delta \dot{u} + \dot{w} \delta \dot{w}) - I_1 \left(\frac{\partial \dot{w}}{\partial x} \delta \dot{u} + \dot{u} \frac{\partial \delta \dot{w}}{\partial x} \right) + I_2 \left(\frac{\partial \dot{w}}{\partial x} \frac{\partial \delta \dot{w}}{\partial x} \right) \\ &+ I_3 \left(\frac{\partial \dot{w}}{\partial x} \delta \dot{u} - \dot{\phi} \delta \dot{u} + \dot{u} \frac{\partial \delta \dot{w}}{\partial x} - \dot{u} \delta \dot{\phi} \right) + I_4 \left(\dot{\phi} \frac{\partial \delta \dot{w}}{\partial x} - 2 \frac{\partial \dot{w}}{\partial x} \frac{\partial \delta \dot{w}}{\partial x} + \frac{\partial \dot{w}}{\partial x} \delta \dot{\phi} \right) \\ &+ I_5 \left(\frac{\partial \dot{w}}{\partial x} \frac{\partial \delta \dot{w}}{\partial x} - \dot{\phi} \frac{\partial \delta \dot{w}}{\partial x} - \frac{\partial \dot{w}}{\partial x} \delta \dot{\phi} + \dot{\phi} \delta \dot{\phi} \right) \end{aligned} \right\} \quad (10)$$

where I_i ($i = 0, 1, 2, \dots, 5$) are the mass moments of inertia defined as:

$$[I_0, I_1, I_2] = \int_A \rho(z) [1, z, z^2] dA; [I_3, I_4, I_5] = \int_A \rho(z) \Phi(z) [1, z, \Phi(z)] dA \quad (11)$$

Substituting Eqs. (7) and (10) into Eq. (6), and applying the integration-by-parts and collecting the coefficients of δu , δw and $\delta \phi$ lead to the following governing equations of motion:

$$\frac{\partial N_x}{\partial x} = I_0 \ddot{u} - I_1 \frac{\partial \ddot{w}}{\partial x} + I_3 \left(\frac{\partial \ddot{w}}{\partial x} - \ddot{\phi} \right) \quad (12a)$$

$$\frac{\partial P_x}{\partial x} - Q_x = I_3 \ddot{u} - I_4 \frac{\partial \ddot{w}}{\partial x} + I_5 \left(\frac{\partial \ddot{w}}{\partial x} - \ddot{\phi} \right) \tag{12b}$$

$$\frac{\partial^2 P_x}{\partial x^2} - \frac{\partial^2 M_x}{\partial x^2} - \frac{\partial Q_x}{\partial x} = -I_0 \ddot{w} - I_1 \frac{\partial \ddot{u}}{\partial x} + I_2 \frac{\partial^2 \ddot{w}}{\partial x^2} + I_3 \frac{\partial \ddot{u}}{\partial x} + I_4 \left(\frac{\partial \ddot{\phi}}{\partial x} - 2 \frac{\partial^2 \ddot{w}}{\partial x^2} \right) + I_5 \left(\frac{\partial^2 \ddot{w}}{\partial x^2} - \frac{\partial \ddot{\phi}}{\partial x} \right) \tag{12c}$$

The stress resultants given in Eq. (8) are substituted into Eq. (12) to obtain the governing equations of motion in the form of displacements as follows:

$$A_{11} \frac{\partial^2 u}{\partial x^2} - B_{11} \frac{\partial^3 w}{\partial x^3} + C_{11} \left(\frac{\partial^3 w}{\partial x^3} - \frac{\partial^2 \phi}{\partial x^2} \right) = I_0 \ddot{u} - I_1 \frac{\partial \ddot{w}}{\partial x} + I_3 \left(\frac{\partial \ddot{w}}{\partial x} - \ddot{\phi} \right) \tag{13a}$$

$$C_{11} \frac{\partial^2 u}{\partial x^2} - F_{11} \frac{\partial^3 w}{\partial x^3} + H_{11} \left(\frac{\partial^3 w}{\partial x^3} - \frac{\partial^2 \phi}{\partial x^2} \right) - A_{55} \left(\frac{\partial w}{\partial x} - \phi \right) = I_3 \ddot{u} - I_4 \frac{\partial \ddot{w}}{\partial x} + I_5 \left(\frac{\partial \ddot{w}}{\partial x} - \ddot{\phi} \right) \tag{13b}$$

$$C_{11} \frac{\partial^3 u}{\partial x^3} - F_{11} \frac{\partial^4 w}{\partial x^4} + H_{11} \left(\frac{\partial^4 w}{\partial x^4} - \frac{\partial^3 \phi}{\partial x^3} \right) - B_{11} \frac{\partial^3 u}{\partial x^3} + D_{11} \frac{\partial^4 w}{\partial x^4} - F_{11} \left(\frac{\partial^4 w}{\partial x^4} - \frac{\partial^3 \phi}{\partial x^3} \right) - A_{55} \left(\frac{\partial^3 w}{\partial x^3} - \frac{\partial \phi}{\partial x} \right) = -I_0 \ddot{w} - I_1 \frac{\partial \ddot{u}}{\partial x} + I_2 \frac{\partial^2 \ddot{w}}{\partial x^2} + I_3 \frac{\partial \ddot{u}}{\partial x} + I_4 \left(\frac{\partial \ddot{\phi}}{\partial x} - 2 \frac{\partial^2 \ddot{w}}{\partial x^2} \right) + I_5 \left(\frac{\partial^2 \ddot{w}}{\partial x^2} - \frac{\partial \ddot{\phi}}{\partial x} \right) \tag{13c}$$

3. ANALYTICAL SOLUTION

For a FG-CNTRC beam simply-supported at both ends, the Navier solution procedure can be applied to solve this problem. The displacement functions in the form of trigonometric series which satisfy the boundary conditions of the problem are given below:

$$u(x,t) = \sum_{n=1}^{\infty} U_n e^{i\omega t} \cos \alpha x \tag{14a}$$

$$\phi(x,t) = \sum_{n=1}^{\infty} \Phi_n e^{i\omega t} \cos \alpha x \tag{14b}$$

$$w(x,t) = \sum_{n=1}^{\infty} W_n e^{i\omega t} \sin \alpha x \tag{14c}$$

where $i = \sqrt{-1}$; $\alpha = n\pi/L$ is a number of half-wave; U_n , Φ_n and W_n are the unknown parameters and ω is the frequency of free vibration. The displacements in Eq. (14) are substituted into the equations of motion given in Eq. (13) in order to obtain the analytical solutions. The results of the substitution can be arranged into the following matrix form:

$$\begin{pmatrix} s_{11} & s_{12} & s_{13} \\ s_{21} & s_{22} & s_{23} \\ s_{31} & s_{32} & s_{33} \end{pmatrix} - \omega^2 \begin{pmatrix} m_{11} & m_{12} & m_{13} \\ m_{21} & m_{22} & m_{23} \\ m_{31} & m_{32} & m_{33} \end{pmatrix} \begin{pmatrix} U_n \\ \Phi_n \\ W_n \end{pmatrix} = \begin{pmatrix} 0 \\ 0 \\ 0 \end{pmatrix} \tag{15}$$

where the matrix elements of Eq. (15) are given as:

$$\begin{aligned} s_{11} &= -A_{11} \alpha^2, s_{12} = C_{11} \alpha^2, s_{13} = (B_{11} - C_{11}) \alpha^3, \\ s_{21} &= -C_{11} \alpha^2, s_{22} = H_{11} \alpha^2 + A_{55}, s_{23} = (F_{11} - H_{11}) \alpha^3 - A_{55} \alpha, \\ s_{31} &= (C_{11} - B_{11}) \alpha^3, s_{32} = (E_{11} - H_{11}) \alpha^3 - A_{55} \alpha, s_{33} = (D_{11} - 2F_{11} + H_{11}) \alpha^4 + A_{55} \alpha^2 \end{aligned} \tag{16a}$$

$$\begin{aligned}
 m_{11} &= -I_0, m_{12} = I_3, m_{13} = (I_1 - I_3)\alpha, \\
 m_{21} &= -I_3, m_{22} = I_5, m_{23} = (I_4 - I_5)\alpha, \\
 m_{31} &= (I_3 - I_1)\alpha, m_{32} = (I_4 - I_5)\alpha, m_{33} = I_0 + (I_2 - 2I_4 + I_5)\alpha^2
 \end{aligned}
 \tag{16b}$$

Eq. (15) defines an eigenvalue problem with ω_n . The eigenvalues (characteristic values) ω_n are found by setting the determinant of the coefficient matrix in Eq. (15) to zero. The smallest eigenvalue (ω_1) is the fundamental frequency.

4. NUMERICAL RESULTS AND DISCUSSION

In this section, several numerical examples of the free vibration behavior of FG-CNTRC beam are presented. The effective material properties of FG-CNTRC beam at ambient temperature used throughout this paper are given as follows. PMMA is used as the matrix and its material properties are: $E^p = 2.5\text{GPa}$, $\nu^p = 0.3$ and $\rho^p = 1190\text{kg/m}^3$. For reinforcement material, the armchair (10,10) SWCNTs whose properties are: $E_{11}^{CNT} = 600\text{GPa}$, $E_{22}^{CNT} = 10\text{GPa}$, $G_{12}^{CNT} = 17.2\text{GPa}$, $\nu^{CNT} = 0.19$ and $\rho^{CNT} = 1400\text{kg/m}^3$. The dimensionless frequency is defined:

$$\Omega = \omega L \sqrt{I_{00} / A_{110}}
 \tag{17}$$

where A_{110} and I_{00} are A_{11} and I_0 of beam made of pure matrix material, respectively.

Table 1. Comparison of dimensionless fundamental frequencies for FG-CNTRC beams ($L/h=15$, $V_{CNT}^* = 0.12$).

Source	UD	FG-O	FG-X	FG-V
Present	0.9749	0.7446	1.1164	0.9444
Ref. [6]	0.9753	0.7527	1.1150	0.9453

The present frequencies of FG-CNTRC beams are numerically validated by comparing with available frequencies based on the Timoshenko beam theory obtained by Yas and Samadias [6] as shown in table 1. From the comparisons, a close agreement among the results is observed.

Table 2. Dimensionless frequencies for FG-CNTRC beam.

L/h	V_{CNT}^*	Mode 1 ($n=1$)				Mode 3 ($n=3$)			
		UD	FG-O	FG-X	FG-V	UD	FG-O	FG-X	FG-V
10	0.12	1.2596	1.0067	1.3920	1.1275	5.4414	4.7961	5.6523	5.2904
	0.17	1.5700	1.2447	1.7383	1.3920	6.9652	6.1890	7.1835	6.7473
	0.28	1.8279	1.5035	1.9636	1.6464	7.6967	7.1131	7.7749	7.5396
15	0.12	0.9749	0.7446	1.1164	0.8444	4.9512	4.2820	5.2021	4.7057
	0.17	1.1986	0.9081	1.3767	1.0295	6.3071	5.4563	6.6006	5.9549
	0.28	1.4367	1.1145	1.6107	1.3607	7.0286	6.3642	7.1582	6.7371
20	0.12	0.7809	0.5826	0.91287	0.6649	4.5286	3.8060	4.8396	4.2065
	0.17	0.9530	0.70614	1.1171	0.8056	5.7252	4.79027	6.1108	5.2728
	0.28	1.1607	0.8730	1.3362	0.9875	6.4755	5.6679	6.7059	6.0660

The influences of the volume fraction of CNTs (V_{CNT}^*) and the length to thickness ratio (L/h) on the free vibration behavior of the FG-CNTRC beam are showed in table 2. It can be seen that the dimensionless frequency increases with an increase in the volume fraction of CNTs (V_{CNT}^*). And from table 2, it can be observed that the dimensionless frequency decreases as increasing in the length to thickness ratio (L/h). This result is very reasonable because the stiffness of the beam decreases by increasing the length to thickness ratio (L/h). It is also found that the FG-X beam has the highest natural frequency, while the FG-O beam has the lowest natural frequency. Therefore, graded CNTs volume fractions with symmetric distributions through the beam thickness have higher capabilities to reduce or increase the frequency parameter as compared with uniformly and asymmetric distributions.

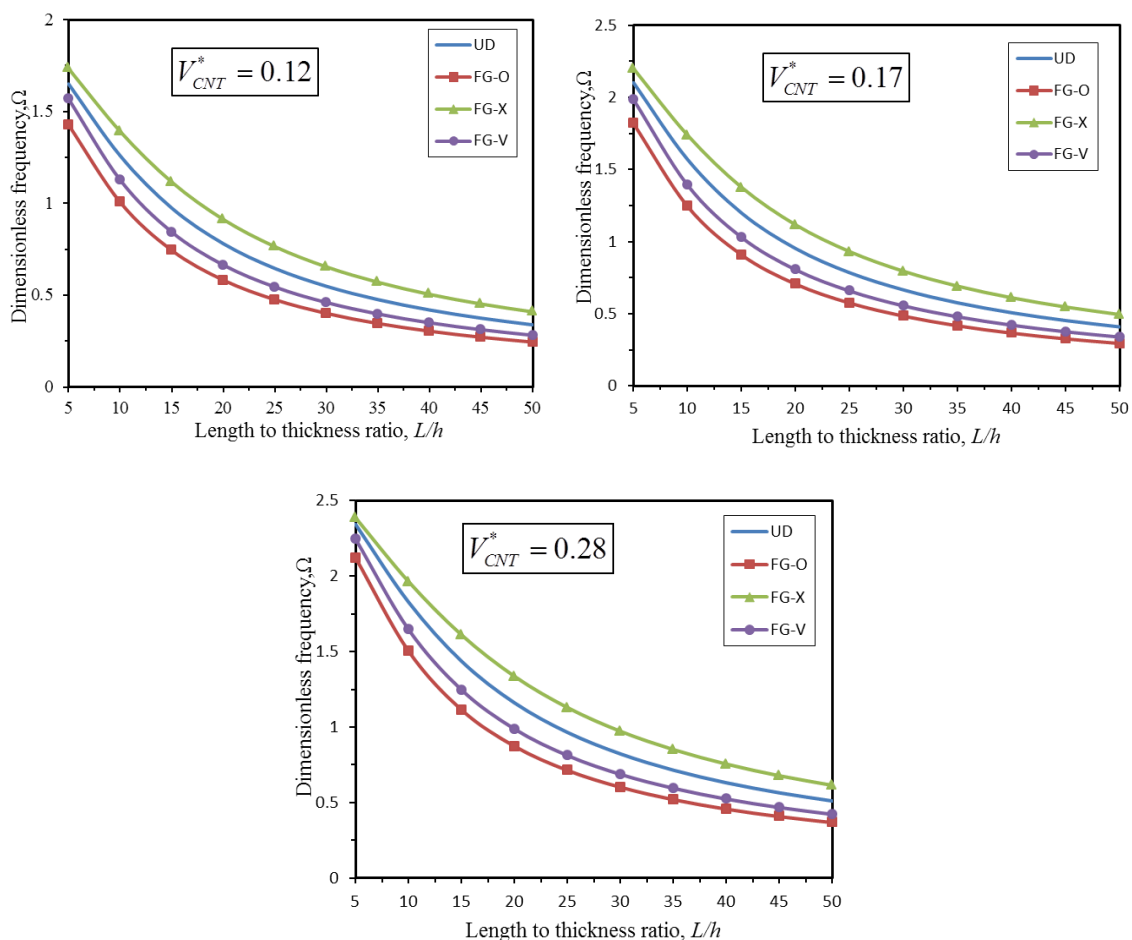


Figure 2. Effect of the length to thickness ratio L/h on the dimensionless frequency.

5. CONCLUSIONS

The trigonometric shear deformation theory is employed to investigate the free vibration problem of simply-supported FG-CNTRC beam. The beam is reinforced by different patterns of CNT distributions in the polymeric matrix. The accuracy of the mathematical model is numerically verified by comparison with some available results. Based on the analysis results, it is found that the FG-X beam has the highest frequency among the different types of FG-CNTRC beams, while the FG-O beam has the smallest frequency.

Acknowledgement: This work is supported by Thai Nguyen University of Technology.

REFERENCES

- [1]. E.T. Thostenson, Z.F. Ren, T.W. Chou, “*Advances in the science and technology of carbon nanotubes and their composites: a review*,” *Composites Science and Technology*, **Vol. 61**, Issue 13, pp. 1899-1912, (2001).
- [2]. K.T. Lau, D. Hui, “*The revolutionary creation of new advanced materials—carbon nanotube composites*,” *Composites Part B: Engineering*, **Vol. 33**, Issue 4, pp. 263–277, (2002).
- [3]. S.H. Shen, “*Nonlinear bending of functionally graded carbon nanotube-reinforced composite plates in thermal environments*,” *Composite Structures*, **Vol. 91**, pp. 9-19, (2009).
- [4]. L.L. Ke, J. Yang, S. Kitipornchai, “*Nonlinear free vibration of functionally graded carbon nanotube-reinforced composite beams*,” *Composite Structures*, **Vol. 92**, Issue 3, pp. 676-683, (2010).
- [5]. M.H. Yas, M. Heshmati, “*Dynamic analysis of functionally graded nanocomposite beams reinforced by randomly oriented carbon nanotube under the action of moving load*,” *Applied Mathematical Modelling*, **Vol. 36**, Issue 4, pp. 1371-1394, (2012).
- [6]. M.H. Yas, N. Samadi, “*Free vibrations and buckling analysis of carbon nanotube-reinforced composite Timoshenko beams on elastic foundation*,” *International Journal of Pressure Vessels and Piping*, **Vol. 98**, pp. 119-128, (2012).
- [7]. N. Wattanasakulpong, V. Ungbhakorn, “*Analytical solutions for bending, buckling and vibration responses of carbon nanotube-reinforced composite beams resting on elastic foundation*,” *Computational Materials Science*, **Vol. 71**, pp. 201–208, (2013).
- [8]. M. Rafiee, J. Yang, S. Kitipornchai, “*Thermal bifurcation buckling of piezoelectric carbon nanotube reinforced composite beams*,” *Computers & Mathematics with Applications*, **Vol. 66**, pp. 1147-1160, (2013).
- [9]. H.S. Shen, Y. Xiang, “*Nonlinear analysis of nanotube-reinforced composite beams resting on elastic foundations in thermal environments*,” *Engineering Structures*, **Vol. 56**, pp. 698-708, (2013).
- [10]. K.M. Liew, Z.X. Lei, L.W. Zhang, “*Mechanical analysis of functionally graded carbon nanotube reinforced composites: A review*,” *Composite Structures*, **Vol. 120**, pp. 90-97, (2015).
- [11]. M. Simsek, J.N. Reddy, “*Bending and vibration of functionally graded microbeams using a new higher order beam theory and the modified couple stress theory*,” *International Journal of Engineering Science*, **Vol. 64**, pp. 37–53, (2013).

TÓM TẮT

Dao động tự do của dầm gia cường ống nano-các bon có cơ tính biến đổi

Mục đích của bài báo này là nghiên cứu ứng xử dao động tự do của dầm gia cường ống nano-các bon có cơ tính biến đổi. Các ống nano-các bon được sắp xếp và phân bố trong pha nền polyme với các kiểu gia cố khác nhau. Các đặc tính vật liệu của dầm gia cường ống nano-các bon có cơ tính biến đổi được ước lượng bằng cách sử dụng quy tắc hỗn hợp. Lý thuyết dầm biến dạng cắt lượng giác được sử dụng để giải quyết vấn đề. Các mô hình toán học được cung cấp trong bài báo này được kiểm chứng bằng cách so sánh với một số kết quả có sẵn. Các kết quả mới về phân tích dao động tự do của dầm gia cường ống nano-các bon có cơ tính biến đổi được trình bày và thảo luận chi tiết. Ảnh hưởng của tỉ số khung hình, tỷ lệ thể tích ống nano-các bon và các kiểu phân bố ống nano-các bon được nghiên cứu.

Từ khoá: Vibration; FG-CNTRC beam; Shear deformation beam theory.